27th International Congress on Sound and Vibration
The annual congress of the International Institute of Acoustics and Vibration (IIAV)
11-16 July, 2021
ICSV27
Annual Congress of the International Institute of Acoustics and Vibration (IIAV)

ASSESSMENT OF TURBULENT PREMIXED COMBUSTION MODELS FOR CH_4/H_2/AIR FLAMES

Halit Kutkan[‡§], Alberto Amato[‡], Giovanni Campa[‡]
[‡]*Ansaldo Energia S.p.A., Genoa, Italy*
[§]*Università degli studi di Genova, Genoa, Italy*
email: halit.kutkan@edu.unige.it

Luis Tay Wo Chong
Ansaldo Energia Switzerland AG, Baden, Switzerland

Eirik Æsøy
Norwegian University of Science and Technology, Trondheim, Norway

This paper presents a comparison of turbulent flame speed based combustion models for CH_4/H_2/air premixed flames including stretch and heat loss effects. It investigates different reaction rate closure expressions in RANS simulations coupled with a turbulent flame speed model recently proposed by the authors. Heat loss and stretch effects are modelled through the tabulation of laminar consumption speeds in a fresh-to-burnt counter flow configuration with detailed chemistry at various heat loss and flame stretch values. Tabulated values are introduced into the models through the turbulent flame speed expression. The performance of each approach is assessed by comparison with OH^* Chemiluminescence images and axial OH^* intensity distributions measured experimentally for atmospheric turbulent premixed bluff-body stabilized CH_4/H_2/air flames ranging from pure methane to pure hydrogen.

Keywords: turbulent premixed combustion, hydrogen enrichment, flame stretch, heat losses, counter flow flames

1. Introduction

Conventional premixed combustion modelling approaches have mainly been developed for fuels like CH_4 or natural gas having unity Lewis number (Le) and may lead to inaccurate results [1] when used for H_2 or H_2 blended ($Le < 1$) fuels. Additionally, reliable modelling requires to consider stretch and heat loss effects in the premixed flame calculations in order to predict the correct flame stabilization [1–4]. In premixed combustion systems, flame stabilization is commonly provided by means of bluff bodies or swirlers. In such configurations, flames stabilize in the inner and outer shear layer zones, and depending on the interplay between heat loss, flame stretch and hydrogen content in the fuel, flames may or may not stabilize in the shear layers producing M-type, V-type or detached-type mean-flame shapes [5,6].

The authors' recent study [1] based on a turbulent flame speed combustion model showed correct prediction of flame stabilization and shape using RANS CFD for atmospheric lean turbulent premixed CH_4/H_2/air flames. The improved prediction is due to the consideration of stretch and heat loss effects

into the model. In this study, the turbulent flame speed expression proposed in [1] is incorporated into 4 different reaction rate source term modelling closures (gradient based TFC and FSC, and algebraic EBU like) in the progress variable transport equation. The performance of each model is assessed by comparing CFD RANS computations with OH^* chemiluminescence data from atmospheric bluff body stabilized turbulent lean premixed CH_4/H_2/air flame experiments ranging from pure methane to pure hydrogen.

The rest of the paper is organised as follows. First, the non-adiabatic and stretched laminar flame speed calculations are presented in section 2.1. The turbulent flame speed model is illustrated in section 2.2. Modelling approaches for the reaction rate source term are described in section 3. The numerical and experimental setups are shown in section 4.1 and 4.2, respectively, as the model results are presented in section 4.3. Finally, conclusions are discussed in section 5.

2. Laminar and turbulent flame speed calculations

2.1 Non-adiabatic and stretched laminar consumption speed calculations

Laminar flame calculations are performed in Cantera 2.4.0 [7] with a fresh-to-burnt counter flow flame configuration under non-adiabatic and stretched conditions. The chemical kinetics is modelled using Aramco-Mech 1.3 [8], while species transport is modelled with a multi-component formulation with Soret effect. Different levels of heat loss β are simulated by decreasing the burnt mixture temperature T_p according to Eq. (1), while keeping the unburnt mixture temperature T_u constant. Flame stretch is evaluated from the maximum velocity gradient at the unburnt side (Eq. (1)), and raised by gradually increasing the flow velocities of burnt and unburnt jets.

$$\beta = \frac{T_p - T_u}{T_{ad} - T_u} \quad , \quad \kappa = max\left|-\frac{\partial u}{\partial x}\right| \tag{1}$$

The flame consumption speed is defined by:

$$S_c = \frac{1}{\rho_u \Delta H_c^o Y_f} \int_{-\infty}^{+\infty} \dot{q}\, dx \tag{2}$$

where ρ_u, ΔH_c^o, Y_f and $\dot{q}$ are the unburnt mixture density, lower heating value, mass fraction of the fuel, and total heat release rate per unit volume, respectively.

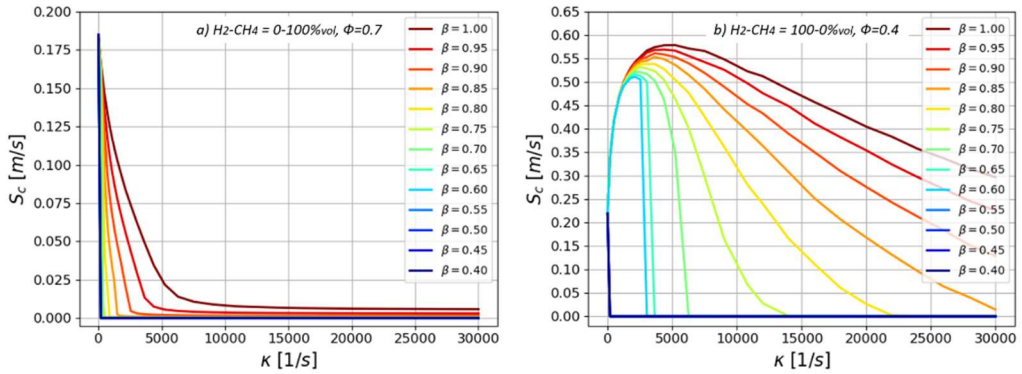

Figure 1: Stretched and non-adiabatic laminar consumption speeds at $P = 1\ atm$ and $T_u = 296\ K$, for a) $0\%\ H_2\ +\ 100\%\ CH_4, \Phi = 0.7$, b) $100\%\ H_2 +\ 0\%\ CH_4, \Phi = 0.4$ mixtures

Fig. 1 shows the consumption speed S_c calculated for the same conditions as the experiments presented later in section 4. The dependence of S_c on κ and β is markedly different between H_2 and CH_4 fuels. For CFD simulations, S_c look-up tables are created for all the mixtures listed in Table 1 (for brevity 2 of them shown in Fig. 1) with varying β and κ in the limits of 1.0-0.4 and 0-30000 1/s, respectively.

2.2 Turbulent flame speed calculation

The turbulent flame speed model used in this study is given below [1]:

$$S_t = S_c + \frac{0.4}{\sqrt{Le^*}} u'^{0.8} S_c^{0.45} \alpha_u^{-0.25} l_t^{0.25} \tag{3}$$

where S_c, Le^*, u', α_u and l_t refer to the non-adiabatic laminar stretched consumption speed, effective Lewis number, turbulent velocity, unburnt thermal diffusivity and turbulent length scale, respectively. The effective Lewis number Le^* is calculated for CH_4/H_2/air mixtures as proposed in [9]:

$$Le^* = \frac{\alpha}{x_{H_2} D_{H_2} + x_{CH_4} D_{CH_4}} \tag{4}$$

where, x_{H_2} and x_{CH_4} are the mole fractions of species in the fuel, D_{H_2} and D_{CH_4} are the binary mass diffusion coefficients with respect to inert N_2 gas, and α is the thermal diffusivity of the mixture. All the transport properties are evaluated at the temperature corresponding to the maximum heat release rate in the 1D unstretched adiabatic laminar flame calculation.

In RANS computations of turbulent flame, stretch (κ) and heat loss (β) are calculated over the computational domain via Eqs. (5) and (6), then depending on their values, consumption speed S_c is interpolated from the look-up tables.

$$\kappa = \underbrace{\left(\delta_{ij} - \widehat{n_i}\widehat{n_j}\right)\frac{\partial \widetilde{u_i}}{\partial x_j}}_{\kappa_{mean}} + \underbrace{\Gamma_K \left(\frac{u'}{S_{L0}}, \frac{L}{\delta_{L0}}\right)\frac{\varepsilon}{k}\left[\frac{1}{Le}(1.76 + \tanh(Le - 2))\right]}_{\kappa_{turb}} \tag{5}$$

$$\beta = 1 - \frac{h_u - \tilde{h}}{\tilde{c} Y_f \Delta H_c^0} \tag{6}$$

In Eq. (5), δ_{ij} is Kronecker delta and $\widehat{n_i}\widehat{n_j}$ is the orientation factor which is calculated as proposed by [10]. $\widetilde{u_i}$ is the Favre averaged velocity component and x_j is the spatial coordinate. Γ_K is the ITNFS (Intermittent Turbulence Net Flame Stretch) efficiency function, and is calculated following [11,12]. u', L, S_{L0}, δ_{L0} are the turbulent velocity, turbulent integral length scale, adiabatic unstretched laminar flame speed and thickness, respectively. k and ε are the turbulent kinetic energy and dissipation rate, and Le is volumetric ratio weighted mixture Lewis number which is calculated following [13]. Further details on the evaluation can be found in [1].

3. Turbulent premixed combustion modelling approaches

In the RANS framework, turbulent premixed combustion can be modelled by solving a Favre averaged transport equation for the combustion progress variable $\tilde{c}$ [14]:

$$\frac{\partial(\bar{\rho}\tilde{c})}{\partial t} + \frac{\partial\left(\bar{\rho}\tilde{u}_j\tilde{c}\right)}{\partial x_j} = \frac{\partial}{\partial x_j}\left(\bar{\rho} D_t \frac{\partial \tilde{c}}{\partial x_j}\right) + \bar{\dot{\omega}} \tag{7}$$

where ρ, t, u_j, x_j, D_t, and $\bar{\dot{\omega}}$ are the density, time, velocity component, spatial direction, turbulent diffusivity (ratio of turbulent kinematic viscosity to turbulent Schmidt number, $D_t = \nu_t / Sc_t$), and reaction rate source term, respectively. In Eq. (7), $\bar{\dot{\omega}}$ term is responsible for the turbulence chemistry interaction and can be modelled as being function of turbulent flame speed S_t. In the following subsections, the different reaction rate source term models investigated in this paper, are presented.

3.1 ExtH₂TFC model

Originally, the TFC (Turbulent Flame Speed Closure) model was developed by Zimont et al. and the reaction source term is modelled as [14]:

$$\bar{\dot{\omega}} = \rho_u S_t |\nabla \tilde{c}| \tag{8}$$

where the magnitude of gradient of progress variable $\tilde{c}$ is calculated by:

$$|\nabla \tilde{c}| = \left\{ \sum_{j=1}^{3} \left(\frac{\partial \tilde{c}}{\partial x_j} \right)^2 \right\}^{0.5} \tag{9}$$

The only difference between ExtH$_2$TFC model and the original TFC model is that S_t is calculated from Eq. (3), instead of Zimont's original S_t expression [14]. Eq. (3) was calibrated against lean premixed CH$_4$/H$_2$/air flames under atmospheric pressure [1], has Lewis number dependency for hydrogen's high diffusivity and takes into account stretch and heat loss effects through the consumption speed S_c.

3.2 ExtH₂FSC model

The FSC (Flame Speed Closure) model was developed by Lipatnikov et al. [15] based on Zimont's TFC model [14] to better reproduce the flame brush development. According to this model, D_t in Eq. (7) is replaced by $D_{t,t}$ while S_t in Eq. (8) is replaced by $S_{t,t}$ as defined below [15]:

$$D_{t,t} = D_t \left[1 - exp\left(-\frac{t_{fd}}{\tau'} \right) \right], \quad S_{t,t} = S_t \left\{ 1 + \frac{\tau'}{t_{fd}} \left[exp\left(-\frac{t_{fd}}{\tau'} \right) - 1 \right] \right\}^{0.5} \tag{10}$$

The flame development time t_{fd} and the fully developed flame time scale τ' terms, used in Eq. (10), are defined as:

$$t_{fd} = \frac{x_c - x_{fh}}{u_{dump}}, \quad \tau' = \frac{D_t}{u'^2} \tag{11}$$

where x_c is the axial coordinate of the cell of interest, x_{fh} is the axial coordinate of the flame holder (bluff body top surface in Fig. 2 a), and u_{dump} is the axial mean velocity at the dump plane.

3.3 ExtH₂KPP model

The ExtH$_2$KPP model is derived from the Schmid model [16]. In his study, Schmid first focused on deriving an analytical expression for the turbulent flame speed S_t, and then applied KPP (Kolmogorov-Petrovski-Piskunov) theory [12] to derive the following expression for the reaction source term $\bar{\dot{\omega}}$:

$$\bar{\dot{\omega}} = C \rho_u \frac{S_t^2}{u'^2} \frac{\varepsilon}{k} \tilde{c}(1 - \tilde{c}) \tag{12}$$

In Eq. (12), differently from [16], the turbulent flame speed S_t of Eq. (3) is utilized and the model constant was calibrated to best match the flame length of the mixture with 56.6% H$_2$ + 43.4% CH$_4$ in section 4, resulting in $C = 2.5$.

3.4 ExtH₂LV model

In the limit of infinitely thin premixed flames under the flamelet assumption, the reaction rate source term is assumed to have relation $\bar{\dot{\omega}} \equiv \rho_u S_t |\nabla \tilde{c}| \equiv \rho_u \langle S_c \rangle \Sigma$ [17]. Assuming an average flame consumption speed $\langle S_c \rangle \approx S_{L0}$, and modelling the flame surface density Σ from fractal theories [12,18], Lindstedt and Vaos derived the following closure:

$$\bar{\dot{\omega}} = C_R \rho_u \frac{S_{L0}}{V_K} \frac{\varepsilon}{k} \tilde{c}(1-\tilde{c}) \tag{13}$$

In Eq. (13), C_R is a model coefficient, S_{L0} is the unstretched adiabatic laminar flame speed, V_K is the Kolmogorov velocity scale $V_K = (\varepsilon\nu)^{0.25}$, and ν, ε and k are the molecular kinematic viscosity, turbulence dissipation rate and turbulent kinetic energy respectively. Muppala et al. [19] calibrated the model coefficient as $C_R = 4.0/e^{Le^*-1}$, and obtained results in agreement with experimental data for adiabatic premixed CH_4/H_2/air flames. In this study, it is proposed to replace $C_R S_{L0}$ by S_t (Eq. (3)) obtaining the following reaction rate source term (labelled "ExtH_2LV model"):

$$\bar{\dot{\omega}} = \rho_u \frac{S_t}{V_K} \frac{\varepsilon}{k} \tilde{c}(1-\tilde{c}) \tag{14}$$

4. Experimental and CFD results

4.1 Experimental setup

Figure 2 a) shows the experimental setup. The combustor has been operated with 5 different mixtures of CH_4/H_2/air premixed gas, ranging from pure methane to pure hydrogen (see Table 1). Air and fuel are mixed a meter before the plenum entrance in order to provide the fully premixed condition at room temperature. The flame is stabilized by a bluff-body supported by a centre rod, producing a blockage ratio of 47%. Images of OH^* Chemiluminescence were captured using a Phantom V2012 (LaVision IRO) camera, with a Cerco 2178 UV 100F/2.8 lens equipped with 310 ± 10 nanometer band pass filter. The planar view was obtained using a 3 point Abel deconvolution. Further information on the experimental set-up are available in [5].

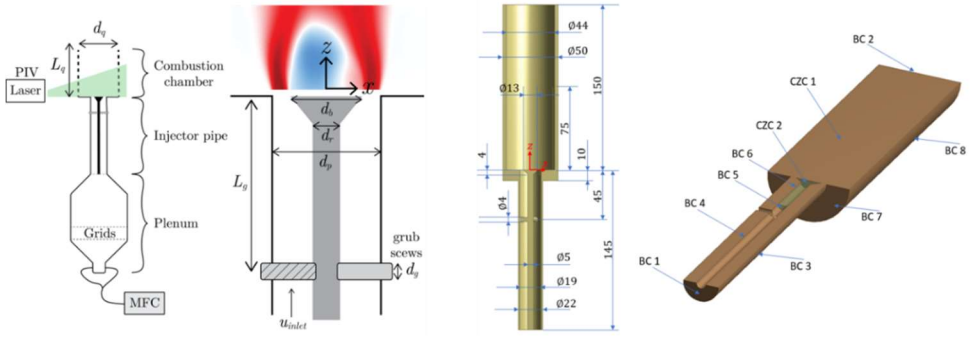

a) Atmospheric single sector test rig b) Section view of burner CAD geometry and computational domain

Figure 2: Single sector atmospheric test rig schematical view (measurements are in mm)

4.2 CFD calculations

CFD studies were carried out in Ansys Fluent 2019 R3 on the 3D geometry. The progress variable $\tilde{c}$ equation (Eq. (7)) was solved using the non-adiabatic partially premixed combustion setup with chemical equilibrium chemistry model. Since the cases are perfectly premixed, equations of mixture fraction and its variance were disabled in the solution process. Reynolds stress turbulence model was chosen and the combustion models were introduced via user defined functions (UDFs). Velocity inlet and pressure outlet boundary conditions were applied with the values listed in Table 1. For combustion chamber dump plane and side surfaces (BC 7 and BC 8 in Fig. 2b), shell conduction wall BC is assigned with the wall thicknesses and heat transfer coefficients (HTC) stated in Table 1 with ambient temperature of 296 K. Bluff body (CZC 2 in Fig. 2 b)) is modelled as a solid domain and thermal coupled wall BC is applied. Further information on the computational setup is available in [1].

Table 1: Experiment and numerical model conditions

$P[kW]$	$V_{H_2}[\%]$	$\Phi[-]$	$u_{in}[m/s]$	$P_{out}[Pa]$	$T_{in}[K]$	$BC\ 7\ wall\ BC$	$BC\ 8\ wall\ BC$
7	0	0.7	11.8	101325	296	t=10mm, HTC=8.6 W/m^{2}K	t=3mm, HTC=150 W/m^{2}K
7	25.2	0.7	11.8	101325	296	t=10mm, HTC=8.6 W/m^{2}K	t=3mm, HTC=150 W/m^{2}K
7	56.6	0.7	11.5	101325	296	t=10mm, HTC=8.6 W/m^{2}K	t=3mm, HTC=150 W/m^{2}K
7	67	0.7	11.4	101325	296	t=10mm, HTC=8.6 W/m^{2}K	t=3mm, HTC=150 W/m^{2}K
7	100	0.4	17.1	101325	296	t=10mm, HTC=8.6 W/m^{2}K	t=3mm, HTC=150 W/m^{2}K

4.3 Reactive flow results

In Fig. 3, the heat release rate (HRR) contours in the mid-section plane obtained from the CFD computations are compared to the experimentally measured normalized Abel deconvoluted OH^* chemiluminescence contours. Axial HRR distributions (Fig. 4) are plotted considering that the integral of the distributions from the CFDs should be equal to those from experiments.

As observed from Fig. 3, all models (except ExtH_2KPP at 25.2% H_2) could correctly capture the mean flame shape and transition from V flame to M flame (between 0% H_2 and 56.6% H_2) for all the cases. This shows that the proposed S_t expression, Eq. (3), works well for these experiment conditions. For the 25.2% H_2 case with ExtH_2KPP model, the flame could not stabilize, due to a low value of the calibration coefficient C in Eq. (13).

ExtH_2TFC and ExtH_2FSC models predict almost identical flame stabilization shapes, demonstrating that for the cases investigated in this paper the flame brush development terms described in section 3.2 [15] do not significantly affect the predicted HRR distribution. Due to the gradient dependency $|\nabla\tilde{c}|$ in the closure, the ExtH_2TFC and ExtH_2FSC models, predict thinner flame brush thicknesses than observed in the experiments. Instead, the ExtH_2KPP and ExtH_2LV models predict flame brush thickness distribution closer to the experiments due to the $\tilde{c}(1-\tilde{c})$ terms. Additionally, ExtH_2TFC and ExtH_2FSC models predict almost zero heat release at the flame tip and maximum heat release at the flame attaching points at the wall.

Although all the models show stronger quenching than the experiments at the outer shear layers, the ExtH_2KPP model predicts even stronger flame quenching than all the other models. This is due to different dependence of ExtH_2KPP reaction source term on consumption speed (which is responsible for the modelling of quenching effects) compared to the other models: for ExtH_2KPP $\bar{\dot{\omega}} \propto S_c^{0.9}$, while for the other models $\bar{\dot{\omega}} \propto S_c^{0.45}$.

The best agreements with experiments were achieved with the ExtH_2LV model in both qualitative and quantitative comparisons by means of mean flame shapes (Fig. 3) and axial HRR distributions (Fig. 4).

5. Conclusion

This study investigated a recently proposed turbulent flame speed expression into different reaction rate closure models for CH_4/H_2/air flames in RANS context. The performance of four reaction rate closure models was assessed against experimental measurements of premixed bluff body stabilized flames ranging from pure methane to pure hydrogen. From the comparison, four main conclusions were drawn. First, the S_t expression of Eq. (3) is able to reproduce the transition from M to V flame shapes for increasing hydrogen content for all the investigated closure models, except for the ExtH_2KPP. Second, closure models based on the algebraic expression $\tilde{c}(1-\tilde{c})$ better predicts the flame brush thickness compared to models based on the gradient $|\nabla\tilde{c}|$ expression. The flame brush development terms in the ExtH_2FSC model do not appreciably affect the calculated HRR distribution. Third, all the models show stronger quenching in the outer shear layer compared to the experiments. Finally, among the models tested, the best match with the experimental data is obtained by the ExtH_2LV model.

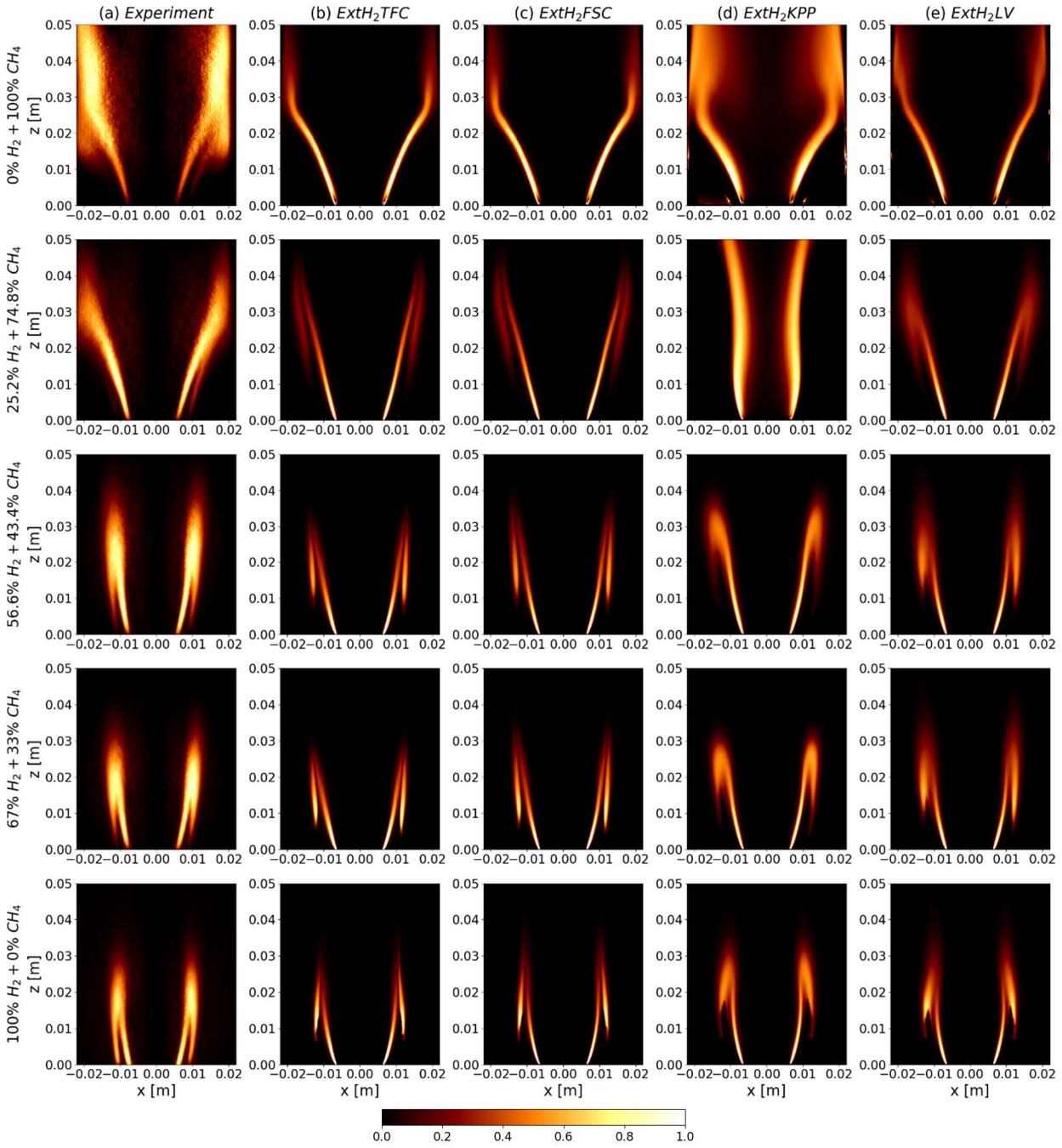

Figure 3: Abel deconvoluted norm. OH^* chemiluminesence vs norm. heat release rate comparison contours

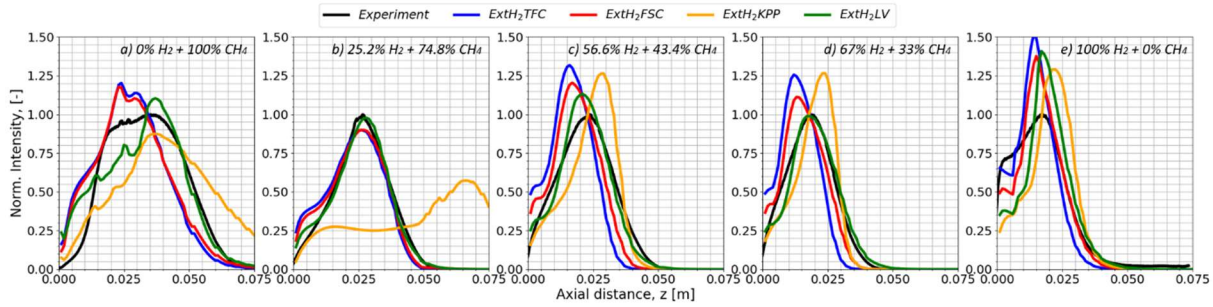

Figure 4: Normalized axial heat release rate distributions

ACKNOWLEDGEMENTS

This work is part of the Marie Skłodowska-Curie Initial Training Network Pollution Know-How and Abatement (POLKA). We gratefully acknowledge the financial support from the European Commission under call H2020-MSCA-ITN-2018 (project number: 813367).

REFERENCES

1 Kutkan, H., Amato, A., Campa, G., Ghirardo, G., Tay-Wo-Chong, L., Æsøy, E. Modelling Of Turbulent Premixed CH_4/H_2/Air Flames Including The Influence of Stretch and Heat Losses, *Proceedings of the ASME Turbo Expo 2021.* GT2021-59063. Virtual Online, June 7-11, 2021.

2 Tay Wo Chong, L., Komarek, T., Zellhuber, M., Lenz, J., Hirsch, C. and Polifke, W. Influence of Strain and Heat loss on Flame Stabilization in a Non-Adiabatic Combustor., *Proceedings of the 4th European Combustion Meeting.* Vienna, AT, April 14-17, 2009.

3 Tay Wo Chong, L., Zellhuber, M., Komarek, T., Im, H. G. and Polifke, W. Combined Influence of Strain and Heat Loss on Turbulent Premixed Flame Stabilization., *Flow, Turbul. Combust.*, **97** (1), 263-294, (2016).

4 Tay Wo Chong, L., Scarpato, A. and Polifke, W. LES Combustion Model With Stretch and Heat Loss Effects for Prediction of Premix Flame Characteristics and Dynamics., *Proceedings of ASME Turbo Expo 2017.* GT2017-63357, V04AT04A029. Charlotte, NC, USA, June 26-30, 2017.

5 Æsøy, E., Aguilar, J. G., Wiseman, S., Bothien, M. R., Worth, N. A. and Dawson, J. R., Scaling and prediction of transfer functions in lean premixed H2/CH4-flames., *Combust. Flame*, **215**, 269-282, (2020).

6 Guiberti, T. F., Durox, D., Scouflaire, P. and Schuller, T. Impact of heat loss and hydrogen enrichment on the shape of confined swirling flames., *Proc. Combust. Inst.*, **35** (2), 1385-1392, (2015).

7 Goodwin, D. G., Speth, R. L., Moffat, H. K. and Weber, B. W. Cantera: An object-oriented software toolkit for chemical kinetics, thermodynamics, and transport processes., available: https://www.cantera.org, Version 2.4.0.

8 Metcalfe, W. K., Burke, S. M., Ahmed, S. S. and Curran, H. J. A hierarchical and comparative kinetic modeling study of C1 - C2 hydrocarbon and oxygenated fuels., *Int. J. Chem. Kinet.*, **45**, 638-675, (2013).

9 Dinkelacker, F., Manickam, B. and Muppala, S. P. R. Modelling and simulation of lean premixed turbulent methane/hydrogen/air flames with an effective Lewis number approach., *Combust. Flame*, **158** (9), 1742-1749, (2011).

10 Veynante, D., Piana, J., Duclos, J. M. and Martel, C. Experimental analysis of flame surface density models for premixed turbulent combustion., *Symposium (International) on Combustion*, **26** (1), 413-420, (1996).

11 Meneveau, C. and Poinsot, T. Stretching and quenching of flamelets in premixed turbulent combustion., *Combust. Flame*, **86** (4), 311-332, (1991).

12 Poinsot, T. and Veynante, D. *Theoretical and Numerical Combustion.* 3rd edition by Poinsot and Veynante, Bordeaux (2012).

13 Bougrine, S., Richard, S., Colin, O. and Veynante, D. Fuel composition effects on flame stretch in turbulent premixed combustion: Numerical analysis of flame-vortex interaction and formulation of a new efficiency function., *Flow, Turbul. Combust.*, **93**, 251-289, (2014).

14 Zimont, V., Polifke, W., Bettelini, M. and Weisenstein, W. An efficient computational model for premixed turbulent combustion at high reynolds numbers based on a turbulent flame speed closure., *J. Eng. Gas Turbines Power*, **120** (3), 526-532, (1997).

15 Lipatnikov, A. N. and Chomiak, J. Turbulent flame speed and thickness: phenomenology, evaluation, and application in multi-dimensional simulations., *Prog. Energy Combust. Sci.*, **28** (1), 1-74, (2002).

16 Schmid, H. P., Habisreuther, P. and Leuckel, W. A model for calculating heat release in premixed turbulent flames., *Combust. Flame*, **113** (1-2), 79-91, (1998).

17 Vervisch, L. and Veynante, D. Interlinks between approaches for modeling turbulent flames., *Proc. Combust. Inst.*, **28** (1), 175-183, (2000).

18 Lindstedt, R. P. and Váos, E. M. Modeling of premixed turbulent flames with second moment methods., *Combust. Flame*, **116** (4), 461–485, (1999).

19 Muppala, S. P. R., Manickam, B. and Dinkelacker, F. A comparative study of different reaction models for turbulent methane/hydrogen/air combustion., *J. Therm. Eng.*, **1** (5), 367–380, (2015).